



HAL
open science

A Comprehensive Set of Juno In Situ and Remote Sensing Observations of the Ganymede Auroral Footprint

V. Hue, J. R. Szalay, T. K. Greathouse, B. Bonfond, S. Kotsiaros, C. K. Louis, A. H. Sulaiman, G. Clark, F. Allegrini, G. R. Gladstone, et al.

► **To cite this version:**

V. Hue, J. R. Szalay, T. K. Greathouse, B. Bonfond, S. Kotsiaros, et al.. A Comprehensive Set of Juno In Situ and Remote Sensing Observations of the Ganymede Auroral Footprint. *Geophysical Research Letters*, 2022, 49 (7), pp.e2021GL096994. 10.1029/2021GL096994 . insu-03667435

HAL Id: insu-03667435

<https://insu.hal.science/insu-03667435>

Submitted on 16 May 2022

HAL is a multi-disciplinary open access archive for the deposit and dissemination of scientific research documents, whether they are published or not. The documents may come from teaching and research institutions in France or abroad, or from public or private research centers.

L'archive ouverte pluridisciplinaire **HAL**, est destinée au dépôt et à la diffusion de documents scientifiques de niveau recherche, publiés ou non, émanant des établissements d'enseignement et de recherche français ou étrangers, des laboratoires publics ou privés.

Copyright

Geophysical Research Letters®

RESEARCH LETTER

10.1029/2021GL096994

Key Points:

- Juno crossed the magnetic flux tube connected to Ganymede auroral footprint and recorded a multi-instrument set of measurements
- Juno measured ~ 316 mW/m² of precipitating electrons while magnetically tied to Ganymede's leading auroral footprint spot
- The associated Juno measurements suggest that it transited through a region linked to the transhemispheric electron beam

Supporting Information:

Supporting Information may be found in the online version of this article.

Correspondence to:

V. Hue,
vhue@swri.edu;
vhue@swri.org

Citation:

Hue, V., Szalay, J. R., Greathouse, T. K., Bonfond, B., Kotsiaros, S., Louis, C. K., et al. (2022). A comprehensive set of Juno in situ and remote sensing observations of the Ganymede auroral footprint. *Geophysical Research Letters*, 49, e2021GL096994. <https://doi.org/10.1029/2021GL096994>

Received 11 NOV 2021

Accepted 9 FEB 2022

Author Contributions:

Conceptualization: A. H. Sulaiman
Data curation: C. K. Louis, G. Clark, F. Allegrini
Formal analysis: J. R. Szalay
Funding acquisition: G. R. Gladstone, S. J. Bolton, J. E. P. Connerney
Investigation: G. Clark, C. Paranicas, A. Mura, A. Moirano, D. J. Gershman, M. W. Davis, R. W. Ebert, J.-C. Gérard, R. S. Giles, D. C. Grodent, M. Imai, J. A. Kammer, W. S. Kurth, L. Lamy, B. H. Mauk
Methodology: B. Bonfond, A. H. Sulaiman
Project Administration: F. Allegrini
Resources: J. R. Szalay, M. W. Davis
Software: J. R. Szalay, T. K. Greathouse, M. H. Versteeg

A Comprehensive Set of Juno In Situ and Remote Sensing Observations of the Ganymede Auroral Footprint

V. Hue¹ , J. R. Szalay² , T. K. Greathouse¹ , B. Bonfond³ , S. Kotsiaros⁴ , C. K. Louis⁵ , A. H. Sulaiman⁶ , G. Clark⁷ , F. Allegrini^{1,8} , G. R. Gladstone^{1,8} , C. Paranicas⁷ , M. H. Versteeg¹ , A. Mura⁹ , A. Moirano⁹ , D. J. Gershman¹⁰ , S. J. Bolton¹, J. E. P. Connerney^{10,11} , M. W. Davis¹ , R. W. Ebert^{1,8} , J.-C. Gérard³ , R. S. Giles¹ , D. C. Grodent³ , M. Imai¹² , J. A. Kammer¹ , W. S. Kurth⁶ , L. Lamy^{13,14} , and B. H. Mauk⁷

¹Southwest Research Institute, San Antonio, TX, USA, ²Department of Astrophysical Sciences, Princeton University, Princeton, NJ, USA, ³STAR Institute, LPAP, Université de Liège, Liège, Belgium, ⁴National Space Institute Measurement and Instrumentation Systems, DTU, Kongens Lyngby, Denmark, ⁵School of Cosmic Physics, DIAS Dunsink Observatory, Dublin Institute for Advanced Studies, Dublin, Ireland, ⁶Department of Physics and Astronomy, University of Iowa, Iowa City, IA, USA, ⁷Johns Hopkins University Applied Physics Laboratory, Laurel, MD, USA, ⁸University of Texas at San Antonio, San Antonio, TX, USA, ⁹Institute for Space Astrophysics and Planetology, National Institute for Astrophysics, Rome, Italy, ¹⁰NASA Goddard Spaceflight Center, Greenbelt, MD, USA, ¹¹Space Research Corporation, Annapolis, MD, USA, ¹²Department of Electrical Engineering and Information Science, National Institute of Technology (KOSEN), Niihama College, Niihama, Japan, ¹³LESIA, Observatoire de Paris, Université PSL, CNRS, Sorbonne Université, Université de Paris, Meudon, France, ¹⁴LAM, Pythéas, Aix Marseille Université, CNRS, CNES, Marseille, France

Abstract Jupiter's satellite auroral footprints are a manifestation of the satellite-magnetosphere interaction of the Galilean moons. Juno's polar elliptical orbit enables crossing the magnetic flux tubes connecting each Galilean moon with their associated auroral emission. Its payload allows measuring the fields and particle population in the flux tubes while remotely sensing their associated auroral emissions. During its thirtieth perijove, Juno crossed the flux tube directly connected to Ganymede's leading footprint spot, a unique event in the entire Juno prime mission. Juno revealed a highly-structured precipitating electron flux, up to 316 mW/m², while measuring both a small perturbation in the magnetic field azimuthal component and small Poynting flux with an estimated total downward current of 4.2 ± 1.2 kA. Based on the evolution of the footprint morphology and the field and particle measurements, Juno transited for the first time through a region connected to the transhemispheric electron beam of the Ganymede footprint.

Plain Language Summary The interaction between Jupiter's corotating plasma torus and the Galilean satellites generates a set of complex magnetospheric processes. One such interaction produces permanent auroral spots around Jupiter's northern and southern poles, known as footprints. For each close flyby, Juno's in situ instruments can measure such interaction. During its thirtieth perijove, Juno crossed the magnetic field lines connecting the interaction region of Ganymede with one of its auroral spots on Jupiter. This study describes and analyzes the set of measurements associated with that unique event.

1. Introduction

The Io plasma torus around Jupiter is composed of iogenic material brought to corotation by Jupiter's magnetic field. It then forms the plasma sheet, which is confined in the centrifugal equator near the magnetic equator. Because Jupiter's magnetic dipole is tilted from its rotation axis, the plasma sheet sweeps through the Galilean satellites twice every ~ 10 -hr rotation period. In the frame attached to the plasma sheet, the satellites travel up and down the sheet, experiencing denser plasma conditions there.

The satellites act as obstacles to the corotating plasma, generating strong electrodynamic interactions (e.g., Kivelson et al., 2004; Thomas et al., 2004; Saur et al., 2004, and others). Such interactions induce magnetic perturbations that travel along the magnetic field lines as Alfvén waves toward Jupiter and ultimately lead to the auroral footprints on Jupiter's atmosphere (e.g., Clarke et al., 2004).

Compared to the other moons, the interaction at Io is amplified by the stronger background Jovian magnetic field. The Hubble Space Telescope (HST) previously helped understanding the morphology of the Io footprint and how it changes with Io's centrifugal latitude (Bonfond et al., 2008; J.-C. Gérard et al., 2006). Jones and Su (2008)

Supervision: G. R. Gladstone
Validation: T. K. Greathouse
Writing – original draft: J. R. Szalay, T. K. Greathouse, B. Bonfond, C. K. Louis, A. H. Sulaiman, F. Allegrini
Writing – review & editing: J. R. Szalay, T. K. Greathouse, B. Bonfond, C. K. Louis, A. H. Sulaiman, F. Allegrini, R. S. Giles, W. S. Kurth

found that when the Alfvén waves generated in the Io interaction region reach high latitudes, they may sustain a large parallel electric field that accelerates electrons both planetward and antiplanetward. The planetward electrons trigger the Main Alfvén Wing (MAW) auroral spot, and the antiplanetward ones lead to the transhemispheric electron beam (TEB) spot on the opposite hemisphere (Bonfond et al., 2008). Additionally, the Alfvén waves may be partly reflected and transmitted by the plasma density gradients encountered along the wave path, such as the plasma sheet boundaries or Jupiter's ionosphere (Neubauer, 1980; Goertz, 1980), creating a complex auroral spot and tail pattern modulated by the Io's centrifugal latitude (Bonfond, 2012; Bonfond et al., 2013; Bonfond, Saur, et al., 2017).

Ganymede possesses an internally driven magnetic field, creating a magnetosphere embedded into the larger Jovian magnetosphere and therefore acting as a larger obstacle to the corotating plasma sheet than its physical size. Past HST campaigns showed that the Ganymede auroral footprint surface matches a region 8–20 Ganymede radius wide (R_G) around Ganymede and revealed its footprint multiplicity, suggesting that similar physics than at Io is controlling the morphology of the Ganymede footprint (Bonfond et al., 2013; Grodent et al., 2009).

The Juno mission, in a polar elliptical orbit around Jupiter, provides a unique opportunity to study the moon-magnetosphere interaction (Bolton et al., 2017). Juno crosses at least once per orbit the magnetic flux tubes connecting each Galilean satellite, or their region downstream of the plasma flow, with Jupiter. Its instrument suite allows the in situ characterization of that interaction by measuring the field and particle population in the flux tubes while remotely sensing the associated infrared (IR) and ultraviolet (UV) auroral emissions on Jupiter. Depending on how far Juno crosses the flux tubes downstream the plasma flow from the moon, its instruments probe the physics responsible for the footprint or tail emission.

Juno brought a wealth of discoveries on the physics responsible for the Io, Europa, and Ganymede auroral footprints. Juno's in situ instruments showed that the broad, power law-like, electron energy distribution leading to the Io footprint tail is consistent with an Alfvénic acceleration process (Damiano et al., 2019; Szalay et al., 2018). These observations, combined with the evidence of sustained Alfvénic wave activity throughout the Io footprint tail, as well as the Alfvén waves turbulent cascade resulting in electron energization (Gershman et al., 2019; Sulaiman et al., 2020), settle the debate on the processes responsible for the tail emission (e.g., Bonfond, Saur, et al., 2017; Delamere et al., 2003).

Unlike most Io crossings, measurements connected to the Europa footprint tail showed signs of an electron distribution resulting at least in part from electrostatic acceleration processes, with enhanced precipitating electrons in the 0.38–25 keV range (Allegrini, Gladstone, et al., 2020). Evidence for Alfvénic acceleration was observed during a Ganymede tail crossing (Szalay et al., 2020a), showing (a) broadband electrons with precipitating fluxes of ~ 11 mW/m² and enhanced flux in the 0.5–40 keV range, (b) a strong magnetic Alfvénic perturbation with associated Poynting flux of ~ 100 mW/m², that is, ~ 10 times the precipitating electron energy flux (EF) measured by Juno's in situ instruments, and (c) strong associated decametric emissions (Louis et al., 2020).

On 8 November 2020, Juno crossed the flux tube magnetically connected to the leading Ganymede footprint in Jupiter's southern hemisphere, an event that only occurred once for Ganymede during Juno's prime mission. This work describes the associated set of Juno measurements. A description of the instruments is first provided, followed by the description of the event, concluded by an interpretation and discussion.

2. Instrument Description

Juno's remote sensing instruments were designed to provide context UV and IR imaging of the auroral regions while the particle and field instruments perform in situ measurements of the charged particle populations, magnetic field, and electromagnetic waves responsible for these auroral emissions (Bolton et al., 2017).

The Ultraviolet Spectrograph (UVS; Gladstone, Persyn, et al. (2017)) is a photon-counting imaging spectrograph operating in the 68–210 nm range (Davis et al., 2011; Greathouse et al., 2013; Hue, Gladstone, et al., 2019). As Juno is a spin-stabilized spacecraft, UVS records one spin worth of Jupiter's data every 30 s. UVS possesses a scan mirror that allows its field of regard to be shifted up to $\pm 30^\circ$ away from the spin plane. Juno's spinning nature combined with UVS' mirror pointing flexibility allows building up complete maps of Jupiter's aurora by coadding consecutive swaths of data. Previous UVS measurements were used to correlate the auroral UV brightness

with Juno's in situ particle instruments (e.g., Allegrini, Mauk, et al., 2020; Ebert et al., 2019; Gladstone, Versteeg, et al., 2017; J. C. Gérard et al., 2019; Li et al., 2017; Mauk et al., 2020), measure variations in the Io footprint brightness during solar eclipses (Hue, Greathouse, et al., 2019), characterize transient emission features in Jupiter's auroral region (Bonfond et al., 2021; Bonfond, Gladstone, et al., 2017; Giles et al., 2020; Haewsantati et al., 2020; Giles et al., 2021; Hue et al., 2021), as well as monitor Jupiter's radiation environment (Bonfond et al., 2018; Kammer et al., 2019).

The Jovian Auroral Distributions Experiment (JADE; McComas et al., 2017) is composed of two electron sensors and one ion sensor. The electron sensors, JADE-E, measure electrons in the 0.05–100 keV range. Each sensor has a 120° FOV in azimuth (i.e., Juno's spin plane) and has deflectors to track the direction of the magnetic field up to about 35° in elevation for <40-keV electrons and 15° for 100-keV electrons. The Jupiter Energetic Particle Detector Instrument (JEDI; Mauk et al., 2017) is composed of three nearly identical sensors measuring the energy and angular distribution of protons from 10 keV to ~1.5 MeV, ionized oxygen and sulfur up to ~10 MeV, and electrons in the 25–800 keV range. The magnetic field is measured using Juno's fluxgate magnetometer (FGM) (Connerney et al., 2017), and the electromagnetic waves are monitored through the Waves instrument (Kurth et al., 2017). Finally, the Jovian Infrared Auroral Mapper is an IR spectroimager (JIRAM; Adriani et al., 2017), equipped with a L-band filter for auroral imaging, operating between 3.3 and 3.6 μm , which is optimal to observe Jupiter's H_3^+ emission.

3. Description of the Event

Coadded spectral images recorded on 8 November 2020 by UVS over the Ganymede footprint from 02:57:45 to 02:58:45 UTC are shown in Figure 1 as polar projections over the southern hemisphere. The subspot structure seen along the Ganymede footpath can also be observed on a spin-by-spin basis and does not result from a coadding effect of multiple UVS swaths taken at different times (see also Figure S1 in Supporting Information S1). Panel D shows the UV-brightness distribution along the Ganymede footpath plotted as a function of the Ganymede system III W-longitude (λ_G hereafter) and offset by the λ_G location of the leading spot λ_G^0 , such that $\Delta\lambda_G = \lambda_G - \lambda_G^0$. Note that all quoted longitudes here are in the SIII W-longitude system. λ_G corresponds to the instantaneous field-line tracing from a point along the Ganymede footpath to the satellite orbital plane, considering the JRM09 magnetic field model combined with a current sheet model (Connerney et al., 1981, 2018). In order to maximize the signal-to-noise ratio, the UV brightness is calculated using the photons recorded in the 115–118 nm and 125–165 nm range and multiplied by 1.84 to extrapolate to the total $\text{H}_2 + \text{Lyman-}\alpha$ emissions in the 75–198 nm range, following Hue et al. (2021).

UVS observations reveal one leading spot followed by one secondary, dimmer spot, a diffuse tail, and a third spot (Figure 1c). The spacing along the Ganymede footpath between the leading and secondary spot is $2,200 \pm 166$ km ($\Delta\lambda_G = 7.5^\circ \pm 0.3^\circ$) while the spacing between the secondary and third spots is $2,300 \pm 298$ km ($\Delta\lambda_G = 9.0^\circ \pm 1.1^\circ$). Unlike Io, the Europa- and Ganymede-related auroral footprints do not always show a diffuse tail (Bonfond, Saur, et al., 2017); however, on this occasion, a tail is observed.

Data recorded by JADE, MAG, and Waves are displayed in Figure 2, showing the electron differential energy flux summed in within the downward loss cone (Figure 2a), the electron pitch angles (PA) distribution (Figure 2b), the precipitating electron EF in the 0.05–40 keV range combined with the MAG data (Figure 2c), and the Waves measurements (Figures 2d and 2e). Because of the gap in the JADE azimuthal field-of-view (FOV) coverage (Figure 2b), only the precipitating electrons were resolved on this particular event.

JADE recorded an enhancement in the precipitating electron EF from 02:55:00 until 02:55:05, showing a double-peaked structure with the first and second peaks up to 316 mW/m² and 58 mW/m², respectively. UVS, on the other hand, cannot resolve the spot's fine structure. The peak UV-brightness associated with the leading spot crossing is 411 ± 42 kR (Figure 1b). Using JRM09, the overall double-peaked structure magnetically maps to a region about $4.4 \pm 0.7 R_G$ ($1 R_G = 2,632$ km), consistent with previous findings (Grodent et al., 2009). The width of the first and second peaks map to a distance of $2.0 \pm 0.7 R_G$, and $1.6 \pm 0.7 R_G$, respectively.

Measurement of the magnetic field perturbation, mainly in the azimuthal B_ϕ component, provides an indication of the presence of field aligned currents (FAC) (e.g., Kotsiaros et al., 2019). Figure 2c displays the perturbation

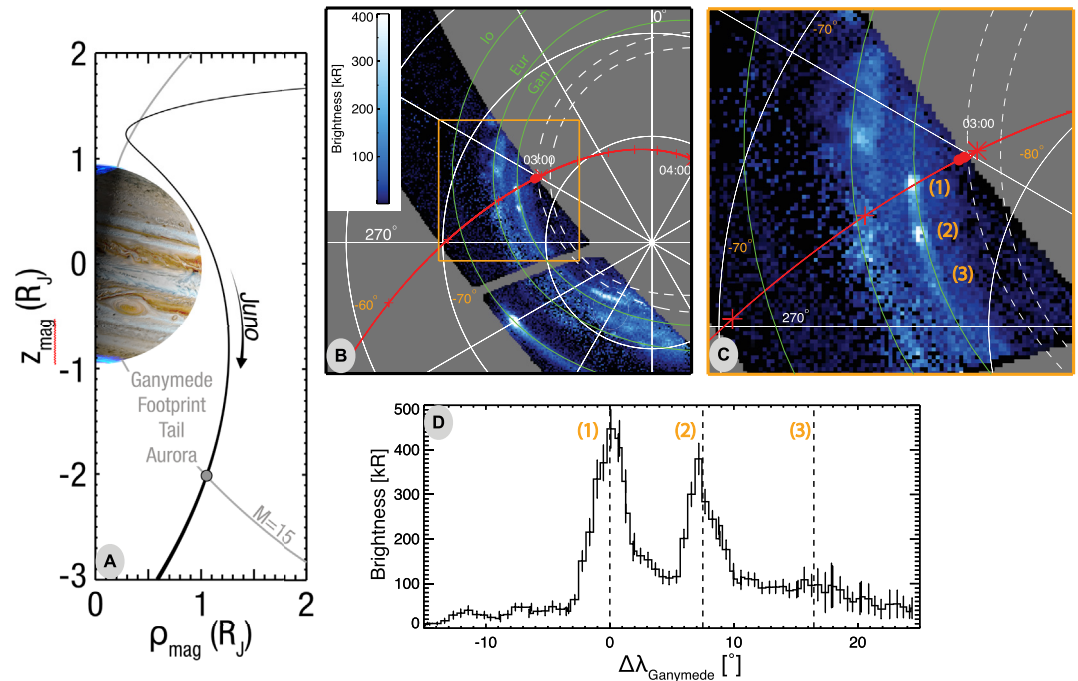


Figure 1. Panel (a) Juno trajectory in the dipole magnetic frame, with +z aligned with the VIP4 magnetic dipole moment, and $\rho_{mag} = \sqrt{x^2 + y^2}$, highlighting Juno's crossing of the field line connected to Ganymede in the South at an altitude of $1.27R_J$. Panel (b) overview of the southern auroral emission recorded by UVS during Juno thirtieth perijove on 8 November 2020 from 02:57:45 to 02:58:45. The Io, Europa, and Ganymede auroral footpaths are highlighted in green while the Juno magnetic footprint track is shown in red using ticks every 10 min, all calculated according to the JRM09 magnetic field + current sheet model (Connerney et al., 1981, 2018). The large red dots along the trajectory show Juno's position when the UVS data were recorded according to JRM09. The dashed line shows the reference oval from Bonfond et al. (2012). Panel (c) zoomed view of the Ganymede auroral footprint. Panel (d) brightness distribution along the Ganymede auroral footpath in a region up to ± 150 km perpendicular to the footprint contour. The brightness peak at $\Delta \lambda_{\text{Ganymede}} = 0^\circ$ corresponds to the leading spot that Juno flew across.

in the magnetic field azimuthal component denoted as δB_ϕ . The perturbations are calculated by removing JRM09 (Connerney et al., 2018) and the latest magnetodisc model (Connerney et al., 2020) from 1-s magnetic field observations. The perturbations are spin-averaged portions (i.e., using a 30-s smoothing function) in order to avoid contamination from low-level spin modulation. MAG shows a ~ 10 nT perturbation in B_ϕ centered around 02:55:02 and shown as a red box in Figure 2c, buried into a larger deflection of about 40 nT in B_ϕ between 02:56 and 03:00 likely associated with the main auroral oval (shown in Figure S2 in Supporting Information S1). MAG shows negligible perturbations in the radial and colatitudinal magnetic field components (not shown here for simplicity, see Figure S2 in Supporting Information S1), implying that the current was purely field-aligned. During the time of interest, Juno flew in a field of about 6×10^4 nT, meaning that the perturbation associated with the crossing is about 0.02% of the background field. The FGM operated at a quantization step size of about 3 nT, indicating that the measured perturbations of ~ 10 nT are well resolved. The ~ 10 nT MAG signature between 02:55:00 and 02:55:04 suggest that Juno crossed a current system composed of upward currents (characterized by $\delta B_\phi > 0$ in the southern hemisphere) followed by downward currents ($\delta B_\phi < 0$) around the time JADE recorded the more pronounced precipitating electron EF, consistent with the southern Alfvén Wing structure (Kivelson et al., 2004). The total downward current can be estimated using Ampere's law. From 02:55:00 and 02:55:04, using Juno trajectory information, the diameter of the Ganymede flux tube Juno passed through is about 170 ± 48 km. This leads to an estimated total downward current of 4.2 ± 1.2 kA. Additionally, the Poynting flux associated with that perturbation can be calculated through the root-mean-square amplitude of the band-pass-filtered magnetic field turbulent fluctuations with cutoff frequencies of 0.2 and 5 Hz, following Gershman et al. (2019). Assuming that the Alfvén speed is equal to the speed of light, the measured Poynting flux recorded during the crossing is ~ 3 mW/m².

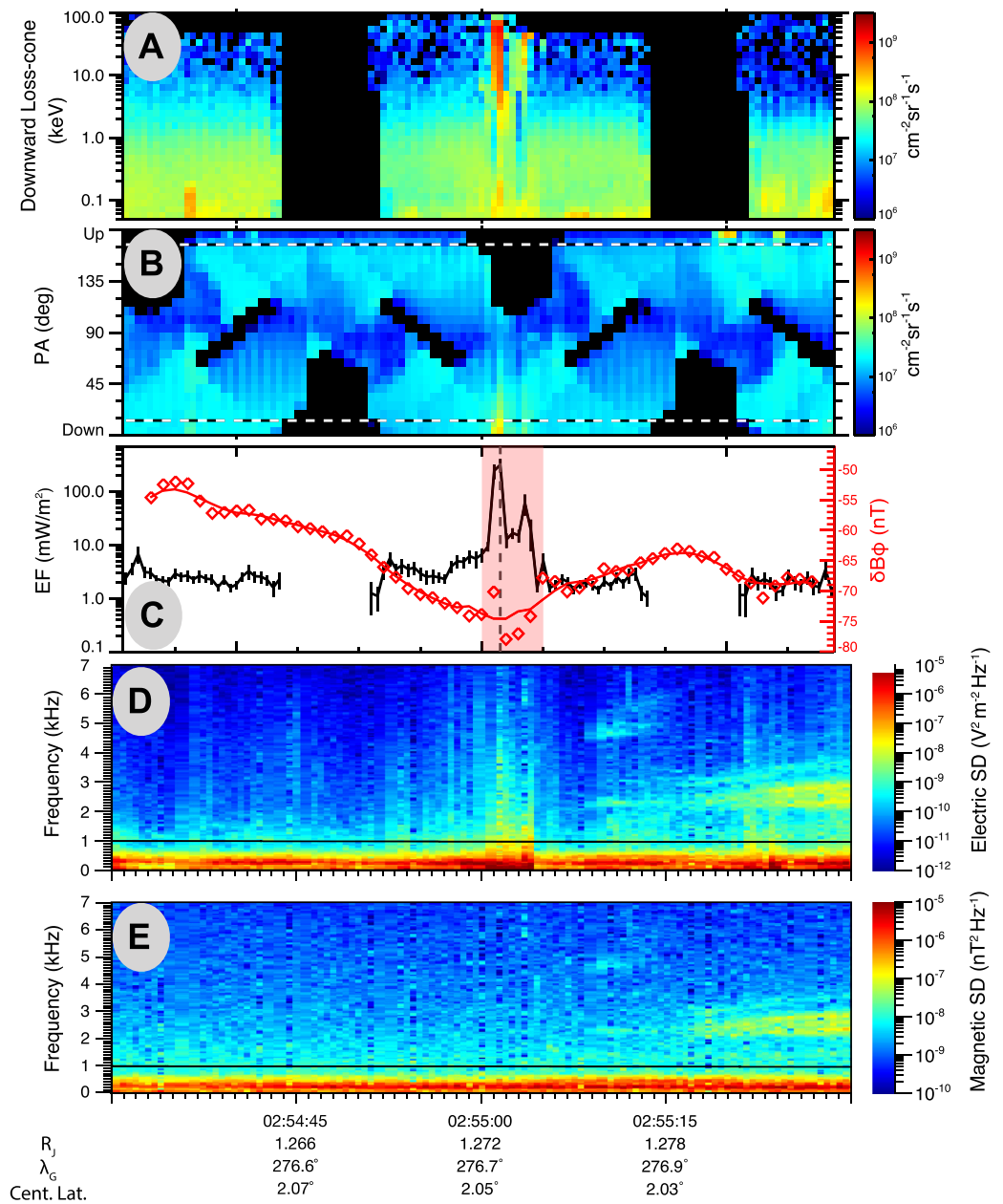


Figure 2. JADE, MAG, and Waves data recorded during the Ganymede flux tube crossing around 02:55:02. Panel A shows the electron differential energy flux integrated within the downward loss cone. Panel B shows the electron pitch angle distribution. Panel C shows the precipitating electron energy flux (black, left axis) with the magnetic field fluctuations (red, right axis) in the azimuthal component δB_ϕ overlaid in red diamonds (1 s cadence) and red line (30 s smoothed). Panels D and E present the Waves measurement. Panel D shows the spectrogram of electric field spectral densities from 0 to 7 kHz while panel E shows the magnetic component of the waves. The black line at about 1 kHz in the two panels is the proton cyclotron frequency f_{cp} . Both panels D and E show a banded emission at about $f_{cp}/2$, likely suggesting ion cyclotron waves. The information at the bottom provides Juno's altitude, as well as Ganymede's SIII W-longitude and centrifugal latitude.

The electric and magnetic field frequency-time spectrograms from Juno/Waves' Low-Frequency Receivers are shown in Figures 2d and 2e. Intense electromagnetic emissions below f_{cp} are present throughout the interval and are likely not related to the Ganymede flux tube crossing. On top of this background, there is a broadband emission that is unique to the flux tube crossing and strongly correlates with the enhancement in electron EF. The intensification in the electric field spectrum with no appreciable power in the magnetic one indicates it is quasia electrostatic. This extends to frequencies above f_{cp} . At higher frequencies (see Figure S3 in Supporting

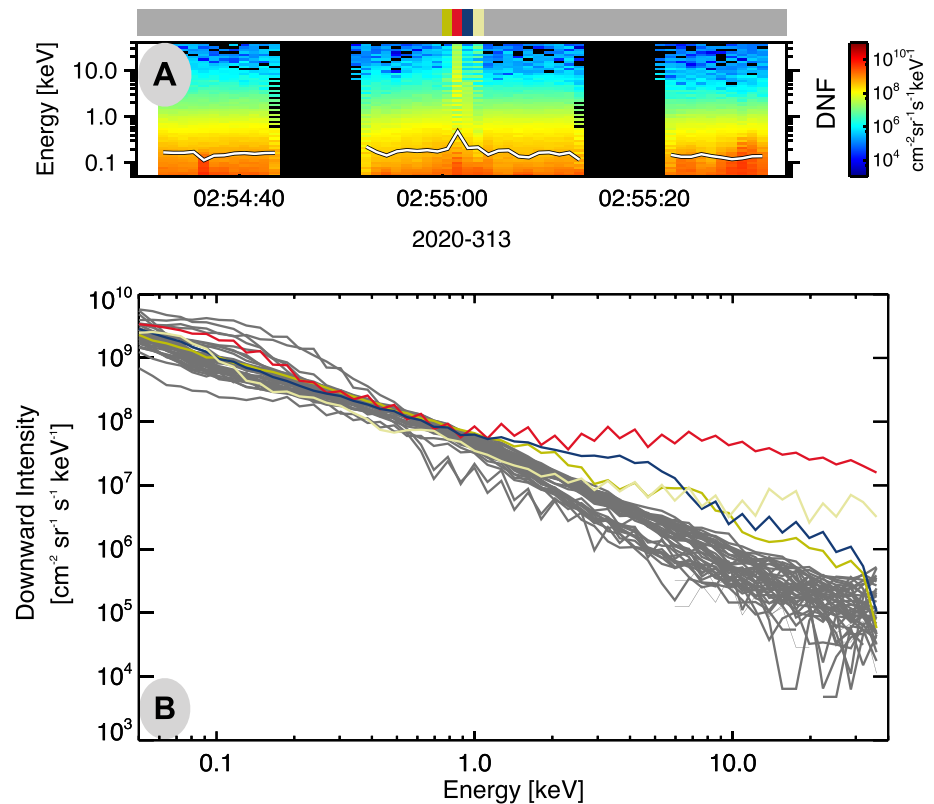


Figure 3. Panel (a) differential energy flux of the precipitating electrons measured by Jovian Auroral Distribution experiment (JADE) integrated for $PA < 20^\circ$. The white line displays the electron characteristic energy. The black areas denote times when the downgoing electrons are outside JADE's field of view and are not sampled. Panel (b) energy spectra of the precipitating electrons at times color-coded according to Panel A's upper ribbon.

Information S1), Waves measured strong intensification at frequencies near the local electron cyclotron frequency f_{ce} around the time of crossing, suggesting Juno may have flown through or near the radio source. From several radio source crossings recorded by Juno, the cyclotron maser instability (CMI) driven by a loss-cone distribution function has been established as a major process at Jupiter to generate hectometric and decametric emissions, induced or not by the Galilean moons (Louarn et al., 2017, 2018; Louis et al., 2020). Following these studies and assuming a loss-cone-driven CMI emission in a weakly relativistic case, the electron energy can be estimated. Around 02:55:02, Waves measured a radio emission in the 1.804–1.894 MHz range while $f_{ce} = 1.786$ MHz. The inferred electron energy is 5.1–28.5 keV, provided that Juno actually flew through the radio source.

The precipitating electron characteristic energy, calculated following Szalay et al. (2020a), shows an enhancement from 0.16 keV prior to the crossing, up to 0.45 keV at the peak of the crossing. JADE measured an enhancement in the electron precipitating flux in the 2–35 keV energy range (Figure 3b). At the crossing itself, JEDI measured a ~ 30 mW/m² flux of >30 keV precipitating electrons when integrating at pitch angles 0–20° (see Figure S4 in Supporting Information S1). JEDI's FOV gap prevents it from sampling the full loss cone population, and the derived electron fluxes are therefore an estimate. The conversion factor from the precipitating electron flux into total unabsorbed H₂ emission is lower than the 10 kR per mW/m² previously derived (see Appendix A of J. C. Gérard et al. (2019)) likely because of the higher assumed characteristic electron energy than measured here, which was previously used to derive that factor (see Figure 12 of Gustin et al., 2016).

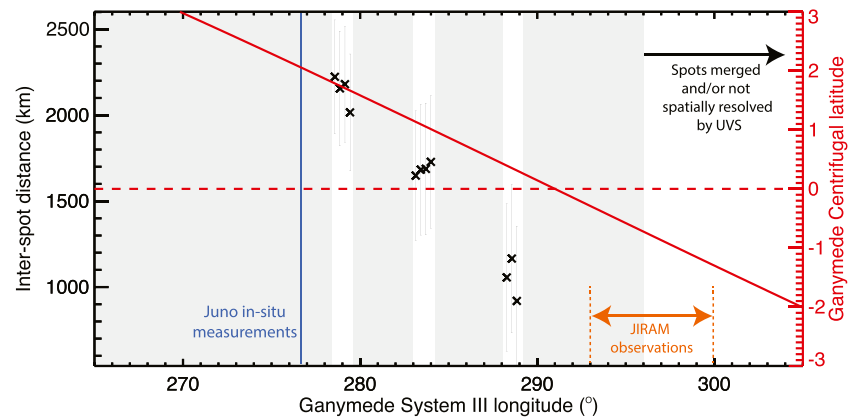


Figure 4. Ganymede footprint interspot (spots 1–2 from Figure 1) distance in kilometers as a function of the Ganymede System III longitude for the PJ30 southern hemisphere observation. The blue line shows the Ganymede longitude at the time of the crossing. The red line shows, on the right axis, the evolution of Ganymede's centrifugal latitude over that Juno pass, as calculated following Phipps and Bagenal (2021). The gray boxes show the coverage gap in the UVS observations. The orange dashed line displays the temporal coverage of the JIRAM observations (see Figure S5 in Supporting Information S1).

4. Interpretation

The Ganymede SIII longitude was 277° at the time of the crossing. This corresponds to a centrifugal latitude of 2° , that is, north of the centrifugal equator, according to the newly derived formulation of the centrifugal equator from Phipps and Bagenal (2021). HST previously observed the multiple spot structure of Ganymede and Europa, consistently with the idea that the physics producing the auroral footprints is common to the Galilean satellites. However, HST only observed the multiple spot structure of Ganymede in a limited longitudinal range, which unfortunately does not overlap with the longitudinal range of the present event (Bonfond, Grodent, et al., 2017). Similarly, only a limited number of JIRAM observations are available in this longitudinal range.

Previously reported Io footprint observations in the $\lambda_{Io} = 200\text{--}300^\circ$ range may help shed light on the expected spot structure (Bonfond, 2012; Bonfond, Saur, et al., 2017; J.-C. Gérard et al., 2006). In the $\lambda_{Io} = 200\text{--}360^\circ$ range, the TEB first leads the MAW, then the two get progressively closer until they merge near $\lambda_{Io} \sim 285^\circ$, as Io is located at the center of the plasma sheet. After that, they split again and the TEB trails behind the MAW (see Figure 4 from Bonfond et al. (2009)). Because of the sparse HST coverage combined with large measurement uncertainties, the RAW-MAW distance was not observed to vary in that longitudinal range. Furthermore, conjugate measurements of the MAW-RAW distance in the north in the $\lambda_{Io} = 0\text{--}100^\circ$ are similarly missing.

UVS measurements of the interspot distance between the first two leading spots on this event are shown in Figure 4. Because UVS builds up a composite auroral image by scanning across and changing the pointing, the Ganymede footprint was not continuously observed over that PJ. Furthermore, Juno's distance to Jupiter evolves quickly past perijove, which degrades UVS's spatial resolution on Jupiter and makes the spots nondiscernible past a certain point. The interspot distance decreases as Ganymede crossed the centrifugal equator from north to south.

Several pieces of information suggest that the leading spot corresponds to the TEB spot and the secondary spot to the MAW, provided that the Io and Ganymede auroral footprints are controlled by similar physics. First, the distance between the TEB and MAW is seen to decrease in the $270\text{--}290^\circ$ range. Although Io's TEB and MAW are expected to merge near $\lambda \sim 285^\circ$, the longitude at which they are observed to merge is known to vary, likely because of the plasma sheet variability, which increases as a function of the radial distance (e.g., Huscher et al., 2021). The amplitude of the field-aligned current was estimated to be 4.2 ± 1.2 kA. Jia et al. (2009) previously estimated the field-aligned current in Ganymede's MAW flux tube to be in the $0.5\text{--}1.2$ MA range, that is, more than 2 orders of magnitude greater than the currents estimated here. The combination of the large recorded number for the electron EF combined with the weak field-aligned current amplitude and the weak Poynting flux would be fully consistent with a TEB crossing.

5. Discussion and Conclusions

During the thirtieth perijove, Juno transited the flux tube connecting Ganymede with Jupiter and mapping to the southern Ganymede auroral footprint. At that time, the Ganymede footprint showed three spots superimposed on a tail of diffuse auroral emission. The UV-brightness of the leading spot was measured to be 411 ± 42 kR, and the set of in situ measurements suggest that Juno transited through a region magnetically connected to that leading spot.

At the crossing time, JADE measured a highly structured energy flux of precipitating electrons characterized by two peaks up to 316 mW/m^2 and 58 mW/m^2 with a broadband increase of precipitating electrons in the 2–35 keV range. This magnitude of precipitating energy fluxes related to moon auroral footprints ($>100 \text{ mW/m}^2$) has only been seen so far for Io during a previous event and interpreted as a MAW crossing (Szalay et al., 2020b; Sulaiman et al., 2020; Gershman et al., 2019). The Juno magnetometer measured a magnetic perturbation $\delta B_\phi \sim 10 \text{ nT}$ indicative of field-aligned currents. In contrast to the reported observations in this work, an earlier Ganymede flux tube crossing further down tail reported an electron energy flux a factor of 24 lower and δB_ϕ 20 times higher (Szalay et al., 2020a).

The quasioleostatic emission that propagates above f_{cp} is consistent with whistler-mode propagation along the resonance cone. This has been observed during flux tube crossings of outer planet satellites, namely, Io and Enceladus (Sulaiman et al., 2018, 2020). A characteristic V-shaped emission is typically observed in a frequency-time spectrogram owing to its dispersion relation, whereby higher frequencies propagate more obliquely to the source magnetic field lines and are detected before and after the flux tube crossing. Unlike previously seen for Io (Sulaiman et al., 2020), this feature is not observed here, likely due to the very short transit time meaning a frequency-time dependence cannot be resolved.

Satellite flux tubes are a source of quasioleostatic whistler-mode waves due to the presence of field-aligned currents. These waves are generated by a beam-plasma instability via the Landau resonance (Farrell et al., 1988). It is therefore likely that these waves are directly associated with the observed electron beams. The Landau resonance condition requires both the waves and beam to travel in the same direction; therefore, we propose that these waves are also downgoing. This would suggest that their source is not local to Juno and some distance away, which would support the diffuse, rather than well-structured, spectral character of the emission.

The evolution of the interspot distance combined with the weak field-aligned current amplitude and the weak Poynting flux suggests that the leading spot Juno crossed corresponds to the transhemispheric electron beam (TEB) which results from the electron acceleration in the other hemisphere. The generated electron beam can trigger whistler-mode waves via a beam-plasma instability, a scenario consistent with the Waves measurements. Furthermore, the fine structures of both the auroral footprint as revealed by JIRAM and the current systems as revealed by JADE demonstrate that an important part of the moon-magnetosphere interaction still remains unclear and is an active research topic (Mura et al., 2018; Moirano et al., 2021; Szalay et al., 2018, 2020b).

The main conclusions of this work are as follow:

1. Juno flew across the magnetic flux tube connected to the Ganymede auroral footprint and recorded a set of both in situ and remote sensing measurements
2. UVS observations revealed a subspot structure characterized by three auroral spots and a diffuse tail
3. JADE measured a broadband increase of precipitating electrons with fluxes up to 316 mW/m^2 associated with an auroral footprint, an event only outmatched by a previous Io crossing thought to be connected with Io's MAW (PJ12 with fluxes $\sim 600 \text{ mW/m}^2$)
4. The perturbation in the magnetic field azimuthal component of $\sim 10 \text{ nT}$ was surprisingly small given the magnitude of the electron flux recorded by JADE, when compared to previous flux tube crossings, and leads to an estimated total downward current of $4.2 \pm 1.2 \text{ kA}$
5. The Poynting flux associated with that perturbation was measured to be $\sim 3 \text{ mW/m}^2$
6. The evolution of the interspot distance combined with the weak measured field-aligned currents and Poynting flux suggest that Juno was connected to Ganymede TEB spot for the first time

Data Availability Statement

All the data used in this study are publicly available on the PDS Atmospheres Node Data Set Catalog https://pds-atmospheres.nmsu.edu/data_and_services/atmospheres_data/JUNO/juno.html, and the PDS Planetary Plasma Interactions (PPI) Node <https://pds-ppi.igpp.ucla.edu/mission/JUNO>.

Acknowledgments

This work is dedicated to Franck Hersant, whose generosity, talent and humbleness was an inspirational force. We are grateful to NASA and contributing institutions that have made the Juno mission possible. This work was funded by the NASA New Frontiers Program for Juno (managed by the Jet Propulsion Laboratory) via a subcontract with Southwest Research Institute. This research was supported through Contract 699041X at the University of Iowa, and through Contract NNM06AA75 C with the Southwest Research Institute at Princeton University. BB, JCG, and DG acknowledge funding for this research by a PRODEX contract of ESA, managed with the help of BELSPO. CL's work at DIAS is supported by the Science Foundation Ireland Grant 18/FRL/6199. LL and CL acknowledge the support from CNES and CNRS/INSU programs of planetology and heliophysics. The work of MI was supported by the JSPS KAKENHI Grant Number JP20K22371.

References

- Adriani, A., Filacchione, G., Di Iorio, T., Turrini, D., Noschese, R., Cicchetti, A., et al. (2017). JIRAM, the Jovian infrared auroral mapper. *Space Science Reviews*, 213, 393–446. <https://doi.org/10.1007/s11214-014-0094-y>
- Allegri, F., Gladstone, G. R., Hue, V., Clark, G., Szalay, J. R., Kurth, W. S., et al. (2020). First Report of electron measurements during a Europa footprint tail crossing by Juno. *Geophysical Research Letters*, 47(18), e89732. <https://doi.org/10.1029/2020GL089732>
- Allegri, F., Mauk, B., Clark, G., Gladstone, G. R., Hue, V., Kurth, W. S., et al. (2020). Energy flux and characteristic energy of electrons over Jupiter's main auroral emission. *Journal of Geophysical Research: Space Physics*, 125(4), e27693. <https://doi.org/10.1029/2019JA026793>
- Bolton, S. J., Adriani, A., Adumitroaie, V., Allison, M., Anderson, J., Atreya, S., et al. (2017). Jupiter's interior and deep atmosphere: The initial pole-to-pole passes with the Juno spacecraft. *Science*, 356, 821–825. <https://doi.org/10.1126/science.aal2108>
- Bonfond, B. (2012). When moons create aurora: The satellite footprints on giant planets. In *Auroral phenomenology and magnetospheric processes: Earth and other planets* (pp. 133–140). American Geophysical Union (AGU). Retrieved from <https://agupubs.onlinelibrary.wiley.com/doi/abs/10.1029/2011GM001169>
- Bonfond, B., Gladstone, G. R., Grodent, D., Gérard, J. C., Greathouse, T. K., Hue, V., et al. (2018). Bar code events in the Juno-UVS data: Signature 10 MeV electron microbursts at Jupiter. *Geophysical Research Letters*, 45(2212), 108–112. <https://doi.org/10.1029/2018GL080490>
- Bonfond, B., Gladstone, G. R., Grodent, D., Greathouse, T. K., Versteeg, M. H., Hue, V., et al. (2017). Morphology of the UV aurorae Jupiter during Juno's first perijove observations. *Geophysical Research Letters*, 44, 4463–4471. <https://doi.org/10.1002/2017GL073114>
- Bonfond, B., Grodent, D., Badman, S. V., Saur, J., Gérard, J.-C., & Radioti, A. (2017). Similarity of the Jovian satellite footprints: Spots multiplicity and dynamics. *Icarus*, 292, 208–217. <https://doi.org/10.1016/j.icarus.2017.01.009>
- Bonfond, B., Grodent, D., Gérard, J. C., Radioti, A., Dols, V., Delamere, P. A., & Clarke, J. T. (2009). The Io UV footprint: Location, inter-spot distances and tail vertical extent. *Journal of Geophysical Research*, 114(A7), A07224. <https://doi.org/10.1029/2009JA014312>
- Bonfond, B., Grodent, D., Gérard, J.-C., Radioti, A., Saur, J., & Jacobsen, S. (2008). UV Io footprint leading spot: A key feature for understanding the UV Io footprint multiplicity? *Geophysical Research Letters*, 35, L05107. <https://doi.org/10.1029/2007GL032418>
- Bonfond, B., Grodent, D., Gérard, J. C., Stallard, T., Clarke, J. T., Yoneda, M., et al. (2012). Auroral evidence of Io's control over the magnetosphere of Jupiter. *Geophysical Research Letters*, 39(1), L01105. <https://doi.org/10.1029/2011GL050253>
- Bonfond, B., Hess, S., Bagenal, F., Gérard, J. C., Grodent, D., Radioti, A., et al. (2013). The multiple spots of the Ganymede auroral footprint. *Geophysical Research Letters*, 40(19), 4977–4981. <https://doi.org/10.1002/grl.50989>
- Bonfond, B., Saur, J., Grodent, D., Badman, S. V., Bisikalo, D., Shematovich, V., et al. (2017). The tails of the satellite auroral footprints at Jupiter. *Journal of Geophysical Research: Space Physics*, 122, 7985–7996. <https://doi.org/10.1002/2017JA024370>
- Bonfond, B., Yao, Z. H., Gladstone, G. R., Grodent, D., Gérard, J.-C., Matar, J., et al. (2021). Are dawn storms Jupiter's auroral substorms? *AGU Advances*, 2(1), e2020AV000275. <https://doi.org/10.1029/2020av000275>
- Clarke, J. T., Grodent, D., Cowley, S. W. H., Bunce, E. J., Zarka, P., Connerney, J. E. P., & Satoh, T. (2004). Jupiter's aurora. In F. Bagenal, T. E. Dowling, & W. B. McKinnon (Eds.), *In: Jupiter: the planet, satellites and magnetosphere*. edited by fran bagenal, timothy e. dowling, william b. mckinnon. *Cambridge planetary science* (Vol. 11, pp. 639–670). Cambridge university press (ISBN: 0-521-81808-7).
- Connerney, J. E. P., Acuna, M. H., & Ness, N. F. (1981). Modeling the Jovian current sheet and inner magnetosphere. *Journal of Geophysical Research*, 86(A10), 8370–8384. <https://doi.org/10.1029/JA086iA10p08370>
- Connerney, J. E. P., Bann, M., Bjarno, J. B., Denver, T., Espley, J., Jorgensen, J. L., et al. (2017). The Juno magnetic field investigation. *Space Science Reviews*, 213(1–4), 39–138. <https://doi.org/10.1007/s11214-017-0334-z>
- Connerney, J. E. P., Kotsiaros, S., Oliverson, R. J., Espley, J. R., Joergensen, J. L., Joergensen, P. S., et al. (2018). A New model of Jupiter's magnetic field from Juno's first nine orbits. *Geophysical Research Letters*, 45, 2590–2596. <https://doi.org/10.1002/2018GL077312>
- Connerney, J. E. P., Timmins, S., Herceg, M., & Joergensen, J. L. (2020). A Jovian magnetodisc model for the Juno Era. *Journal of Geophysical Research: Space Physics*, 125(10), e28138. <https://doi.org/10.1029/2020JA028138>
- Damiano, P. A., Delamere, P. A., Stauffer, B., Ng, C. S., & Johnson, J. R. (2019). Kinetic simulations of electron acceleration by dispersive scale Alfvén waves in Jupiter's magnetosphere. *Geophysical Research Letters*, 46(6), 3043–3051. <https://doi.org/10.1029/2018GL081219>
- Davis, M. W., Gladstone, G. R., Greathouse, T. K., Slater, D. C., Versteeg, M. H., Persson, K. B., et al. (2011). Radiometric performance results of the Juno ultraviolet spectrograph (Juno-UVS). In (Vol. 8146, p. 814604). <https://doi.org/10.1117/12.894274>
- Delamere, P. A., Bagenal, F., Ergun, R., & Su, Y. J. (2003). Momentum transfer between the Io plasma wake and Jupiter's ionosphere. *Journal of Geophysical Research*, 108(A6), 1241. <https://doi.org/10.1029/2002JA009530>
- Ebert, R. W., Greathouse, T. K., Clark, G., Allegri, F., Bagenal, F., Bolton, S. J., et al. (2019). Comparing electron energetics and UV brightness in Jupiter's northern polar region during Juno perijove 5. *Geophysical Research Letters*, 46(1), 19–27. <https://doi.org/10.1029/2018GL081129>
- Farrell, W. M., Gurnett, D. A., Banks, P. M., Bush, R. I., & Raitt, W. J. (1988). An analysis of whistler mode radiation from the spacelab 2 electron beam. *Journal of Geophysical Research*, 93(A1), 153–161. <https://doi.org/10.1029/JA093iA01p0153>
- Gérard, J. C., Bonfond, B., Mauk, B. H., Gladstone, G. R., Yao, Z. H., Greathouse, T. K., et al. (2019). Contemporaneous observations of Jovian energetic auroral electrons and ultraviolet emissions by the Juno spacecraft. *Journal of Geophysical Research: Space Physics*, 124(11), 8298–8317. <https://doi.org/10.1029/2019JA026862>
- Gérard, J.-C., Saqlam, A., Grodent, D., & Clarke, J. T. (2006). Morphology of the ultraviolet Io footprint emission and its control by Io's location. *Journal of Geophysical Research*, 111, A04202. <https://doi.org/10.1029/2005JA011327>
- Gershman, D. J., Connerney, J. E. P., Kotsiaros, S., DiBraccio, G. A., Martos, Y. M., -Viñas, A. F., et al. (2019). Alfvénic fluctuations associated with Jupiter's auroral emissions. *Geophysical Research Letters*, 46(13), 7157–7165. <https://doi.org/10.1029/2019GL082951>
- Giles, R. S., Greathouse, T. K., Bonfond, B., Gladstone, G. R., Kammer, J. A., Hue, V., et al. (2020). Possible transient luminous events observed in Jupiter's upper atmosphere. *Journal of Geophysical Research: Planets*, 125(11), e06659. <https://doi.org/10.1029/2020JE006659>
- Giles, R. S., Greathouse, T. K., Kammer, J. A., Gladstone, G. R., Bonfond, B., Hue, V., et al. (2021). Detection of a Bolidé in Jupiter's atmosphere with Juno UVS. *Geophysical Research Letters*, 48(5), e91797. <https://doi.org/10.1029/2020GL091797>

- Gladstone, G. R., Persyn, S. C., Eterno, J. S., Walther, B. C., Slater, D. C., Davis, M. W., et al. (2017). The ultraviolet spectrograph on NASA's Juno mission. *ssr*, 213, 447–473. <https://doi.org/10.1007/s11214-014-0040-z>
- Gladstone, G. R., Versteeg, M. H., Greathouse, T. K., Hue, V., Davis, M. W., Gérard, J.-C., et al. (2017). Juno-UVS approach observations of Jupiter's auroras. *Geophysical Research Letters*, 44, 7668–7675. <https://doi.org/10.1002/2017GL073377>
- Goertz, C. K. (1980). Io's interaction with the plasma torus. *Journal of Geophysical Research*, 85, 2949–2956. <https://doi.org/10.1029/JA085iA06p02949>
- Greathouse, T. K., Gladstone, G. R., Davis, M. W., Slater, D. C., Versteeg, M. H., Persson, K. B., et al. (2013). Performance results from in-flight commissioning of the Juno ultraviolet spectrograph (Juno-UVS). In *Uv, x-ray, and gamma-ray space instrumentation for astronomy xviii*, 8859. <https://doi.org/10.1117/12.2024537>
- Grodent, D., Bonfond, B., Radioti, A., Gérard, J.-C., Jia, X., Nichols, J. D., & Clarke, J. T. (2009). Auroral footprint of Ganymede. *Journal of Geophysical Research*, 114, A07212. <https://doi.org/10.1029/2009JA014289>
- Gustin, J., Grodent, D., Ray, L. C., Bonfond, B., Bunce, E. J., Nichols, J. D., & Ozak, N. (2016). Characteristics of north jovian aurora from STIS FUV spectral images. *Icarus*, 268, 215–241. <https://doi.org/10.1016/j.icarus.2015.12.048>
- Haesantati, K., Bonfond, B., Wannawichian, S., & Gladstone, G. R. (2020). Jupiter's polar auroral bright spots as seen by Juno-UVS. In *Egu general assembly conference abstracts* (p. 3622).
- Hue, V., Gladstone, G. R., Greathouse, T. K., Kammer, J. A., Davis, M. W., Bonfond, B., et al. (2019). In-flight characterization and calibration of the Juno-Ultraviolet Spectrograph (Juno-UVS). *The Astronomical Journal*, 157(2), 90. <https://doi.org/10.3847/1538-3881/aafb36>
- Hue, V., Greathouse, T. K., Bonfond, B., Saur, J., Gladstone, G. R., Roth, L., et al. (2019). Juno-UVS observation of the Io footprint during solar eclipse. *Journal of Geophysical Research: Space Physics*, 124(7), 5184–5199. <https://doi.org/10.1029/2018JA026431>
- Hue, V., Greathouse, T. K., Gladstone, G. R., Bonfond, B., Gérard, J. C., Vogt, M. F., et al. (2021). Detection and characterization of circular expanding UV emissions observed in Jupiter's polar auroral regions. *Journal of Geophysical Research: Space Physics*, 126(3), e28971. <https://doi.org/10.1029/2020JA028971>
- Huscher, E., Bagenal, F., Wilson, R. J., Allegrini, F., Ebert, R. W., Valek, P. W., et al. (2021). Survey of Juno Observations in Jupiter's Plasma Disk: Density. *Journal of Geophysical Research: Space Physics*, 126(8), e2021JA029446. <https://doi.org/10.1029/2021JA029446>
- Jia, X., Walker, R. J., Kivelson, M. G., Khurana, K. K., & Linker, J. A. (2009). Properties of Ganymede's magnetosphere inferred from improved three-dimensional MHD simulations. *Journal of Geophysical Research*, 114(A9), A09209. <https://doi.org/10.1029/2009JA014375>
- Jones, S. T., & Su, Y. J. (2008). Role of dispersive Alfvén waves in generating parallel electric fields along the Io-Jupiter fluxtube. *Journal of Geophysical Research*, 113(A12), A12205. <https://doi.org/10.1029/2008JA013512>
- Kammer, J. A., Hue, V., Greathouse, T. K., Gladstone, G. R., Davis, M. W., & Versteeg, M. H. (2019). Planning operations in Jupiter's high-radiation environment: Optimization strategies from Juno-ultraviolet spectrograph. *Journal of Astronomical Telescopes, Instruments, and Systems*, 5, 027001. <https://doi.org/10.1117/1.JATIS.5.2.027001>
- Kivelson, M. G., Bagenal, F., Kurth, W. S., Neubauer, F. M., Paranicas, C., & Saur, J. (2004). Magnetospheric interactions with satellites. In F. Bagenal, T. E. Dowling, & W. B. McKinnon (Eds.), *Jupiter: the planet, satellites and magnetosphere* (pp. 513–536).
- Kotsiaros, S., Connerney, J. E. P., Clark, G., Allegrini, F., Gladstone, G. R., Kurth, W. S., et al. (2019). Birkeland currents in Jupiter's magnetosphere observed by the polar-orbiting Juno spacecraft. *Nature Astronomy*, 3, 904–909. <https://doi.org/10.1038/s41550-019-0819-7>
- Kurth, W. S., Hospodarsky, G. B., Kirchner, D. L., Mokrzycki, B. T., Averkamp, T. F., Robison, W. T., et al. (2017). The Juno waves investigation. *Space Science Reviews*, 213, 347–392. <https://doi.org/10.1007/s11214-017-0396-y>
- Li, W., Thorne, R. M., Ma, Q., Zhang, X.-J., Gladstone, G. R., Hue, V., et al. (2017). Understanding the origin of Jupiter's diffuse aurora using Juno's first perijove observations. *Geophysical Research Letters*, 44, 10. <https://doi.org/10.1002/2017GL075545>
- Louarn, P., Allegrini, F., McComas, D. J., Valek, P. W., Kurth, W. S., André, N., et al. (2017). Generation of the Jovian hectometric radiation: First lessons from Juno. *Geophysical Research Letters*, 44(10), 4439–4446. <https://doi.org/10.1002/2017GL072923>
- Louarn, P., Allegrini, F., McComas, D. J., Valek, P. W., Kurth, W. S., André, N., et al. (2018). Observation of electron conics by Juno: Implications for radio generation and acceleration processes. *Geophysical Research Letters*, 45(18), 9408–9416. <https://doi.org/10.1029/2018GL078973>
- Louis, C. K., Louarn, P., Allegrini, F., Kurth, W. S., & Szalay, J. R. (2020). Ganymede-Induced decametric radio emission: In situ observations and measurements by Juno. *Geophysical Research Letters*, 47(20), e90021. <https://doi.org/10.1029/2020GL090021>
- Mauk, B. H., Clark, G., Gladstone, G. R., Kotsiaros, S., Adriani, A., Allegrini, F., et al. (2020). Energetic particles and acceleration regions over Jupiter's polar cap and main aurora: A broad overview. *Journal of Geophysical Research: Space Physics*, 125(3), e27699. <https://doi.org/10.1029/2019JA027699>
- Mauk, B. H., Haggerty, D. K., Jaskulek, S. E., Schlemm, C. E., Brown, L. E., Cooper, S. A., et al. (2017). The Jupiter energetic particle detector instrument (JEDI) investigation for the Juno mission. *Space Science Reviews*, 213(1–4), 289–346. <https://doi.org/10.1007/s11214-013-0025-3>
- McComas, D. J., Alexander, N., Allegrini, F., Bagenal, F., Beebe, C., Clark, G., et al. (2017). The Jovian auroral distributions experiment (JADE) on the Juno mission to Jupiter. *Space Science Reviews*, 213, 547–643. <https://doi.org/10.1007/s11214-013-9990-9>
- Moirano, A., Mura, A., Adriani, A., Dols, V., Bonfond, B., Waite, J. H., & Bolton, S. J. (2021). Morphology of the auroral tail of io, europa, and ganymede from jiram l-band imager. *Journal of Geophysical Research: Space Physics*, 126(9), e2021JA029450. <https://doi.org/10.1029/2021ja029450>
- Mura, A., Adriani, A., Connerney, J. E. P., Bolton, S., Altieri, F., Bagenal, F., et al. (2018). Juno observations of spot structures and a split tail in Io-induced aurorae on Jupiter. *Science*, 361, 774–777. <https://doi.org/10.1126/science.aat1450>
- Neubauer, F. M. (1980). Nonlinear standing Alfvén wave current system at Io—Theory. *Journal of Geophysical Research*, 85, 1171–1178. <https://doi.org/10.1029/JA085iA03p01171>
- Phipps, P., & Bagenal, F. (2021). Centrifugal equator in Jupiter's plasma sheet. *Journal of Geophysical Research: Space Physics*, 126(1), e28713. <https://doi.org/10.1029/2020JA028713>
- Saur, J., Neubauer, F. M., Connerney, J. E. P., Zarka, P., & Kivelson, M. G. (2004). Plasma interaction of Io with its plasma torus. In F. Bagenal, T. E. Dowling, & W. B. McKinnon (Eds.), *Jupiter: the planet, satellites and magnetosphere* (pp. 537–560).
- Sulaiman, A. H., Hospodarsky, G. B., Elliott, S. S., Kurth, W. S., Gurnett, D. A., Imai, M., et al. (2020). Wave-particle interactions associated with Io's auroral footprint: Evidence of Alfvén, ion cyclotron, and whistler modes. *Geophysical Research Letters*, 47(22), e88432. <https://doi.org/10.1029/2020GL088432>
- Sulaiman, A. H., Kurth, W. S., Hospodarsky, G. B., Averkamp, T. F., Ye, S. Y., Menietti, J. D., et al. (2018). Enceladus auroral hiss emissions during cassini's grand finale. *Geophysical Research Letters*, 45(15), 7347–7353. <https://doi.org/10.1029/2018GL078130>
- Szalay, J. R., Allegrini, F., Bagenal, F., Bolton, S. J., Bonfond, B., Clark, G., et al. (2020a). Alfvénic acceleration sustains Ganymede's footprint tail aurora. *Geophysical Research Letters*, 47(3), e86527. <https://doi.org/10.1029/2019GL086527>
- Szalay, J. R., Allegrini, F., Bagenal, F., Bolton, S. J., Bonfond, B., Clark, G., et al. (2020b). A New framework to explain changes in Io's footprint tail electron fluxes. *Geophysical Research Letters*, 47(18), e89267. <https://doi.org/10.1029/2020GL089267>

- Szalay, J. R., Bonfond, B., Allegrini, F., Bagenal, F., Bolton, S., Clark, G., et al. (2018). In situ observations connected to the io footprint tail aurora. *Journal of Geophysical Research: Planets*, *123*(11), 3061–3077. <https://doi.org/10.1029/2018JE005752>
- Thomas, N., Bagenal, F., Hill, T. W., & Wilson, J. K. (2004). The Io neutral clouds and plasma torus. In F. Bagenal, T. E. Dowling, & W. B. McKinnon (Eds.), *Jupiter: the planet, satellites and magnetosphere* (pp. 561–591).